

8 Maosheng N. and Shusheng Z., 2011 "Experimental and Numerical Investigations of Tip Injection on tip Clearance Flow in an Axial Turbine Cascade", Elsevier, Volume 35, Issue 6, Pages 1214-1222.

9 Ahmed M. E., Farouk M. O. and Mabouli A. R., 2013. "Film Cooling Optimization Using Numerical Computation of the Compressible Viscous Flow Equations and Simplex Algorithm", International Journal of Aerospace Engineering, Article ID 859465.

10 Arnal, M.P., 1983. "A General Computer Program for Two-dimensional, Turbulent, Re-circulating Flows", Report No. Fm-83-2.

11 Verestage, H. K., and Malalasekera, W., 1995. "An Introduction to Computational Fluid Dynamic-The Finite volume Method", Longman Group Ltd.

12 Fluent Inc., 2009. Fluent User's Guide, Version 6.3.26.

13 Launder, B.E. and Spalding, D.B., 1972. "Mathematical Models of Turbulence", Academic press, London.

14 Ideriah, F. J. K., 1975, "Review of equation solved in TEACH", private communication.

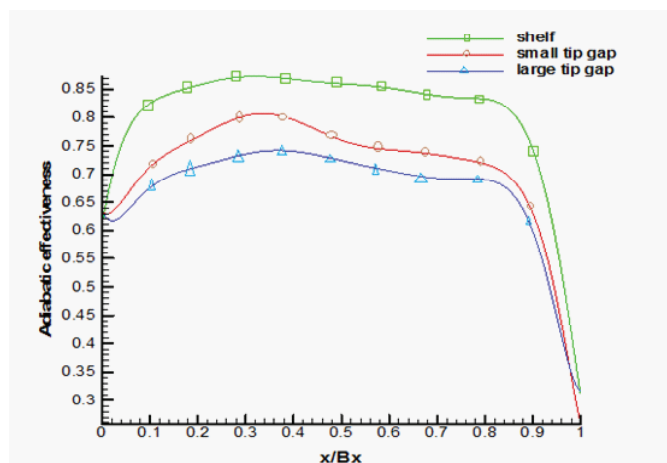


Figure (11) Laterally averaged adiabatic effectiveness for small, large tip gap and shelf.

## 6. CONCLUSIONS

Results show that the effectiveness at small tip gap is better than at large tip gap to reach maximum enhancement 12.6%.

The adiabatic effectiveness increases as the amount of coolant flow increases.

When the shelf is starting of blade and beginning to inter the cooled flow, the blowing ratio is not affected in it.

Finally, the pressure coefficient distribution results show a good agreement with experimental and computational data for Christophel et al.

## 7. REFERENCES

- 1 Metzger, D.E., Bunker, R. S. and Chyu, M.K., 1989, "Cavity Heat Transfer on a Transverse Grooved Wall in a Narrow Flow Channel," ASME Journal of Heat Transfer, Vol. 111, pp. 73-79.
- 2 Jonas, B., 2002, "Internal Cooling of Gas Turbine Blades", PhD, Chalmers university of Technology Goterborg.
- 3 Tallman, J. and Lakshminarayana, B., 2001, " Numerical Simulation of Tip Leakage Flows in Axial Flow Turbines. With Emphasis on Flow Physics Part II: Effect of Outer Casing Relative Motion", Journal of Turbomachinery, 123, pp. 324-333.
- 4 Hohlfeld, E. M., 2003, "Film Cooling Predictions Along the Tip and Platform of a Turbine Blade", Master's Thesis, Virginia Polytechnic Institute and State University, Blacksburg.
- 5 Christophel, J. R., Thole, K. A. and Cunha, F. J., 2005, "Cooling the Tip of a Turbine Blade Using Pressure Side Holes-Part 1: Adiabatic Effectiveness Measurements", ASME paper No. GT2004-53251.
- 6 Adel H. Ayaal, 2005, "Thermal Analysis of a Cooled Turbine Blade", PhD. Thesis, University of Technology.
- 7 Fabien W., Florent D., Gilles L. and Nicolas G., 2010, "3D Simulation of Couple Flow and Solid Heat Conduction For The Calculation of Blade Wall Temperature in a Turbine Stage", ASME paper No. GT2010-22513.

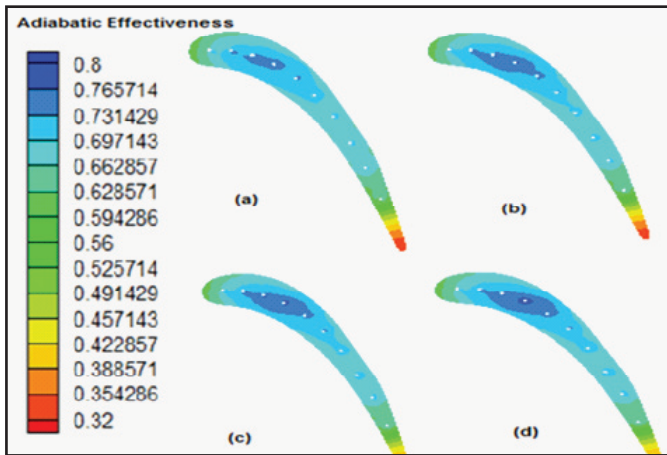


Figure (7) Predictions of adiabatic effectiveness along the tip for the large tip gap with holes blowing at ratios of (a) 0.5%, (b) 1%, (c) 1.5% and (d) 2%.

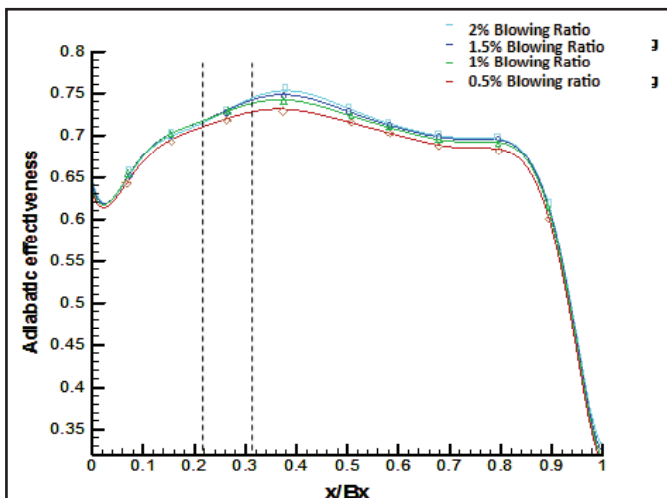


Figure (8) Laterally averaged adiabatic effectiveness for large tip gap at four blowing ratios.

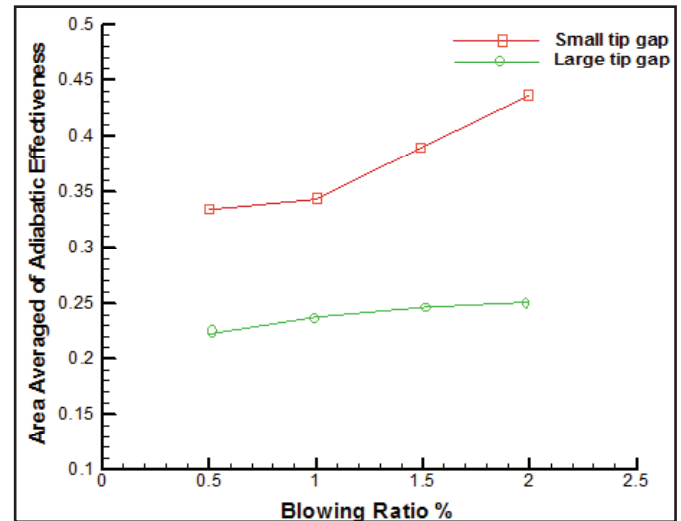


Figure (9) Area averaged of adiabatic effectiveness for two tip gap sizes at different blowing ratio.

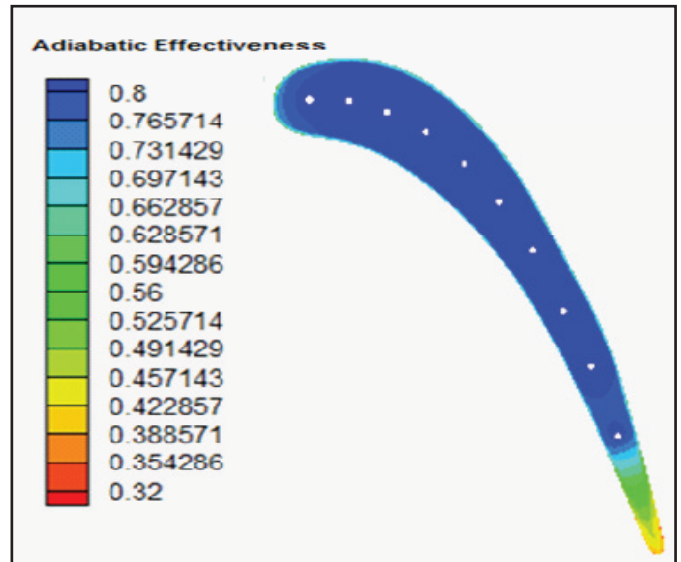


Figure (10) Predictions of adiabatic effectiveness along the shelf.

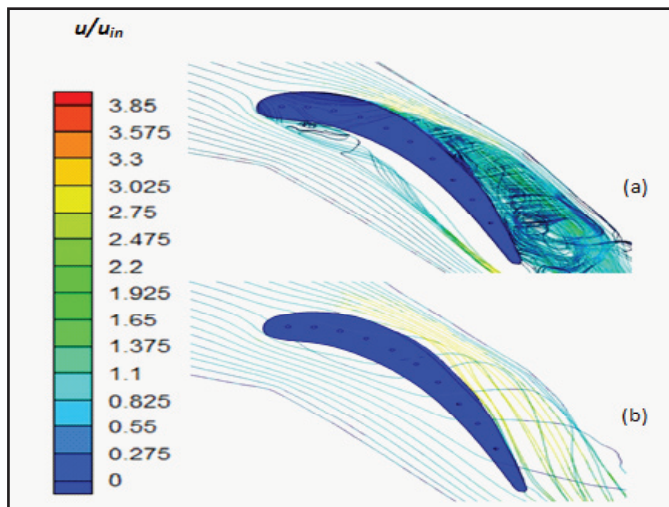


Figure (3) Streamlines released from 1.5 tip gap heights below the shroud that are colored by the non-dimensional spanwise velocity component for film holes blowing with a. a) small tip gap and 1% blowing ratio. and b) large tip gap and 1% blowing ratio.

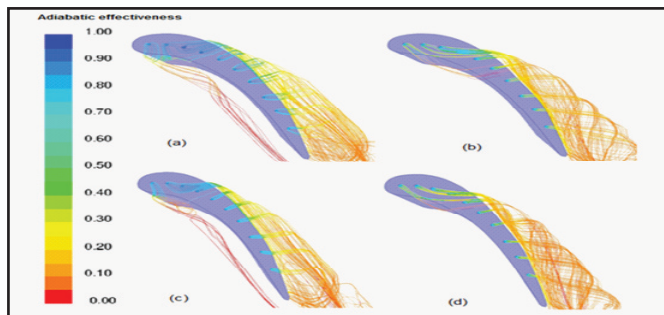


Figure (4) Streamlines colored by non-dimensional temperature released from the film holes for a (a) small tip gap and 2% blowing ratio. (b) large tip gap and 2% blowing ratio. (c) small tip gap and 1% blowing ratio and (d) large tip gap and 1% blowing ratio.

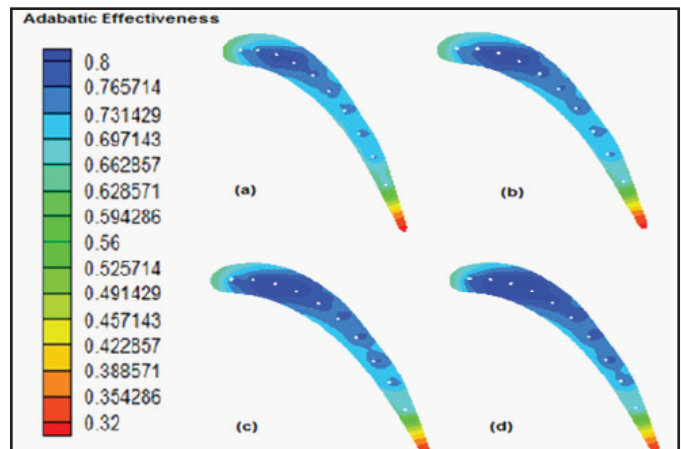


Figure (5) Predictions of adiabatic effectiveness along the tip for the small tip gap with blowing ratios (a) 0.5%, (b) 1%, (c) 1.5% and (d) 2%.

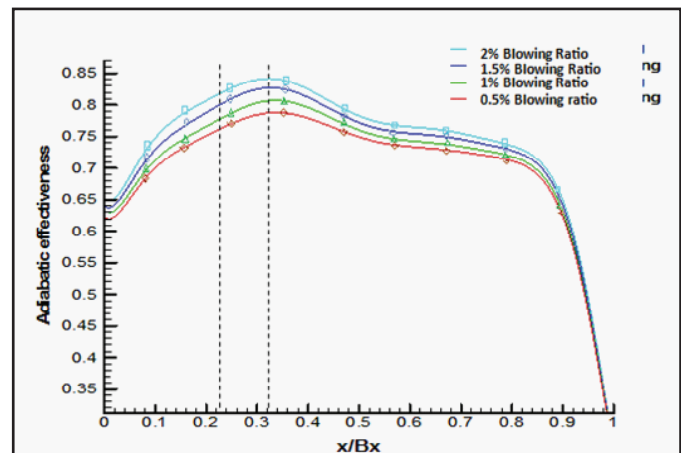


Figure (6) Laterally averaged adiabatic effectiveness for small tip gap at four blowing ratios.

Table (1) Values of constants in the (k- $\epsilon$ ) model at Launder and Spalding 13

$C_\mu$	$C_D$	$C_1$	$C_2$	$\sigma_k$	$\sigma_\epsilon$
0.09	1.0	1.44	1.92	1.0	1.3

Table (2) Special design of geometry and flow condition of the blade.

Parameter	Value
Scaling Factor	12X
Axial Chord, $B_x$	35 cm
True Chord, C	53 cm
Pitch, P	43 cm
Span, S	55.2 cm
Re	2.1E+05
Inlet Angle, $\theta$	16.5°
Blade Angle, °	50°
Small tip gap, h	0.03 cm
Large tip gap, H	0.09 cm

Table (3) Holes locations

Holes	X(cm)	Y(cm)	Diameter(cm)
1	3.43	40.5	0.7
2	6.86	40.43	0.7
3	10.3	39.5	0.7
4	13.7	37.68	0.6
5	17.15	34.91	0.6
6	20.3	31.48	0.6
7	23.2	27.15	0.6
8	26.02	21.857	0.6
9	28.45	16.802	0.6
10	30.88	10.66	0.6

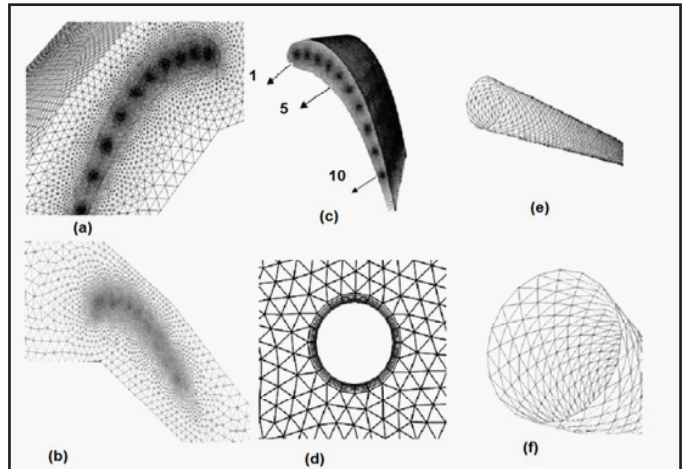


Figure (1) Shows the mesh at (a) duct. (b) shroud. (c) blade. (d) boundary layer mesh around the holes. (e) holes. (f) point at holes edge.

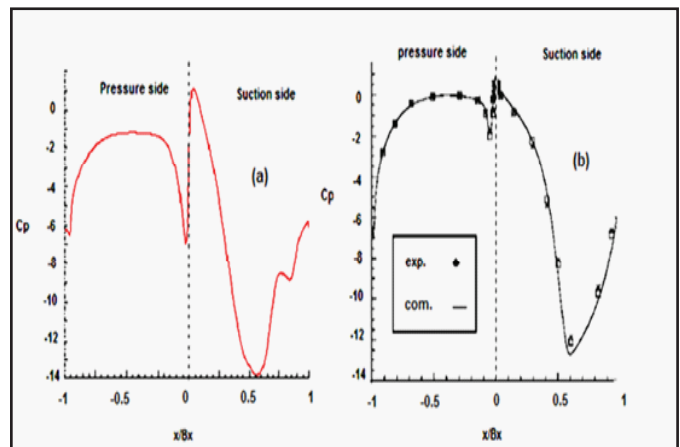


Figure (2) Predicted the static pressure coefficient distributions at suction and pressure side for (a) computational of present study. (b) experimental and computational from Christophel et al. 5

Figure (11) shows the laterally averaged adiabatic effectiveness plot for the large, small tip gap and shelf at blowing ratio of 1%. Figure (11) predicts the adiabatic effectiveness increase at shelf when compare with small and large tip gap, because the shelf is not affected by heat transfer such as the tip and at shelf is starting to inter the cooled flow to blade and it's not affected by heating of blade.

## 5. NOMENCLATURE

Symbol	Description	Dimension
A	Coefficient of the discretized equation, area	m <sup>2</sup>
B <sub>a</sub>	Axial Chord of the blade	m
BR	Blowing ratio $U_w/U_\infty$	---
C	Chord of the blade	m
C <sub>p</sub>	Pressure coefficient $(p-p_{in})/(0.5 \rho v^2)$	---
J	Jacobian of coordinates transformation	---
P	static pressure	Pa
S	Span length	m
S <sub>0</sub>	Source term of $\phi$	---
T	Temperature	°C
u, v, w	Velocity component in x, y, z respectively	m/sec
T <sub>g</sub>	Temperature of hot gases	°C
T <sub>a</sub>	Temperature of cooling air	°C
T <sub>in</sub>	Temperature at the inlet condition	m/sec
T <sub>w</sub>	Temperature at adiabatic wall	°C
u, v, w	Velocity component in x, y, z respectively	m/sec
U <sub>in</sub>	Velocity at inlet conditions	m/sec
U <sub>in</sub>	Velocity of mainstream conditions	m/sec
U <sub>a</sub>	Velocity of coolant conditions	m/sec
x,y,z	Cartesian coordinate	---
<i>Greek Letters</i>		
$\phi$	Dependent variable	---
H	Adiabatic effectiveness, $\eta = (T_w - T_{in}) / (T_g - T_a)$	---
P	Density	Kg/m <sup>3</sup>
E	Rate of dissipation of kinetic energy	m <sup>2</sup> /sec <sup>3</sup>
$\mu$	Dynamic viscosity	N.m/sec <sup>2</sup>
$\frac{\partial}{\partial \xi}, \frac{\partial}{\partial \eta}, \frac{\partial}{\partial \zeta}$	partial derivative in the computational plane	---
<i>Superscript</i>		
C	Coolant conditions	
$\infty$	Mainstream conditions	
<i>Abbreviation</i>		
CFD	Computational Fluid Dynamics	
3D	Three-Dimensional	
SIMPLE	Semi-Implicit Method for Pressure Linked Equation	



is unaffected by blowing from holes. Overall the small tip gap shows higher effectiveness levels than the large tip gap for each blowing ratio. The small tip gap shows that average effectiveness increases with blowing ratio. The small tip gap case shows that the average effectiveness only slightly increases when the blowing ratio is increased from 0.5% to 1%. The reason for this is that at the lowest blowing ratio cooling is provided to the tip because the coolant is injected into the tip gap with a small amount of momentum so that it attaches to the tip surface immediately. At the highest blowing ratio the coolant is injected with so much momentum that it impacts the shroud and turned back to cool the tip surface. At the blowing ratios between these

two extremes, the momentum of the injected coolant is high enough that it cannot initially attach to the tip surface yet low enough that it does not sufficiently impact the shroud to return to the tip. Some of this coolant reattaches to the tip surface further downstream while the rest is lost to the tip leakage flow. Figure (10) predict the adiabatic effectiveness along the shelf. From this figure, a good cooling at large area of shelf and the blowing ratio do not effected on the cooling of the blade because the main hot flow impacts the shelf therefore it will be static and the heat transfer will be decreased. that means the blowing ratio will not affect on the adiabatic effectiveness.

of blowing ratio increases. With the small tip gap, the cooling effectiveness improves as the blowing of coolant is increases from the 0.5% to the 2% blowing case. The averaged effectiveness levels for any blowing ratio are not significantly larger than the other blowing, because tip temperatures can be no lower than the coolant temperature, there is an apparent limit to the amount of cooling that can be gained by increasing the coolant flow from the film holes. The coolant that floods the tip gap is eventually swept away with the tip leakage into the mainstream flow and does not remain in the tip gap past  $x/Bx = 0.85$  to cool regions closer to the trailing edge. This is an important result for the gas turbine industry because the amount of air used to cool the turbine blades has an adverse effect on the overall engine efficiency.

Predicted adiabatic effectiveness drops off substantially when the tip gap is increased to its large height. Figure (7) shows the contours of film holes blowing at a large tip gap. Tip gap leakage at this tip gap height is much greater allowing for significant mixing of the coolant and mainstream gases that results in a reduction of cooling. Tip effectiveness predictions for the large tip gap of Figure (7) do not follow the previous trends seen with the small tip and shrouds at both gap heights. Instead of more coolant increasing the tip cooling, the surface temperatures are predicted to actually maintain the same effectiveness levels or rise

as coolant levels are increased from 0.5% to 2% cooling. Predictions indicate that some of the best cooling occurs for the lowest flow rates of 0.5%. This is due primarily to the low momentum coolant jets that remain attached to the surface of the blade and cool the tip just downstream of the holes. At the higher blowing rates computations suggest hot tip leakage slides between the tip and coolant air to block much of the high velocity coolant jet from mixing out and cooling the region. This phenomena was briefly discussed in Figures (3) and (4) when looking at the flow for a large tip gap.

Figure (8) shows the laterally averaged adiabatic effectiveness plot for the large tip gap. The x-locations of the film holes are labeled with vertical dashed lines. The average effectiveness spikes up at the holes because the areas of the film hole exits are factored into the average as having an effectiveness of 1.0. With the large tip gap, it's not different large in small tip gap only the effectiveness is nearly smallest because the effect of gap. The effectiveness increases with blowing ratio, especially near the holes three and four.

All the adiabatic effectiveness for holes are summarized in Figure (9). Effectiveness values are averaged over the entire area of the blade for each case and then plotted against blowing ratio for both tip gap sizes. The trailing edge region was accounted into the average using effectiveness values of 0 because it



Figures (4 a-b) with the small tip followed by the large tip. Notice that with the small tip, there is an increase in coolant distribution when compared to the larger tip gap. This increased spreading can be explained by a number of factors. Most significant is the effect of the increase in mass flow with a large tip gap. At a large tip gap this leakage serves to dilute the coolant more than would be seen with a smaller gap. This dilution results from high velocity tip leakage flow that has substantial momentum and does not permit holes cooling to penetrate the large gap region as it would the small. The small tip gap has very good coverage over the leading edge. In fact, there is a slight blow-off into the main passage before the cooling flow is pushed into the tip gap near the mid-chord. Reducing the coolant levels (blowing ratio) to 1% as shown in Figure (4 c-d) shows a reduction in the size of the cooling area for both large and small tip cases. This comes as no surprise as a decrease in coolant implies lower velocities and less momentum to block leakage flow.

An astute observer may notice that with a small tip gap the holes flow is shown to cover most of the leading edge and this was confirmed with the streamlines released upstream of the blade. However, the large tip gap streamlines released in Figure (4 b) and Figure (4 d) lead the reader to believe the leading edge region covered by streamlines is cooled,

but this is not true. Looking at Figure (3 b), which depicts a large tip and 1% coolant flow, the streamlines released upstream of the blade penetrate into the leading edge allowing hot gases into the region.

Looking at the tip predictions of Figure (5) shows good tip cooling when coolant levels are at least 1%. As expected additional coolant provides better cooling coverage of the tip, improving from little cooling at 0.5% to almost full leading edge coverage at 2%. The effectiveness contours at the lower blowing ratios (0.5%) show the low momentum cooling jets being swept across the tip along with the hot tip leakage flow. Only as the cooling increases to the previously mentioned 1% is there enough cooling mass and momentum to penetrate upstream into the tip. When the blowing levels are at or above 1% a large region over the blade is cooled to levels approaching  $\eta = 0.8$ , indicating excellent cooling effectiveness. For all cases, the blade tip near the maximum distance between pressure and suction side nearly cooled. The trailing edge is thermally unaffected by the film holes coolant.

Figure (6) shows the laterally averaged adiabatic effectiveness for the small tip gap with all four blowing levels. The peak average effectiveness for the blowing ratios occurs at the same x-location as the three and four holes. Figure (6) shows that the adiabatic effectiveness increases as the amount

adiabatic effectiveness.

Figure (2) shows the pressure coefficient distribution around the blade at midspan for small tip gap in suction and pressure side with the pressure non-dimensionalized by the inlet pressure conditions and given in  $C_p$  parameters. Also this results comparison with experimental and computational data for Christophel et al. [5]. When the air approaching the leading edge of a blade is first slowed down, it then speeds up again as it passes over or beneath the blade. As the velocity changes, so does the dynamic pressure and static pressure according to Bernoulli's principle. Air near the stagnation point has slowed down, and thus the static pressure in this region is higher than the inlet static pressure to main duct. Air that is passing above and below the blade, and thus has speeded up to a value higher than the main inlet path velocity, will produce static pressures that are lower than inlet static pressure. At a point near maximum thickness, maximum velocity and minimum static pressure will occur. Also this figure shows a good agreement with the experimental and computational data for Christophel et al.

Figure (3) depicts streamlines released upstream of the blade at 1.5 tip gaps below the shroud for a blowing ratio 1% and a small and large tip, respectively. In Figure (3a) one can clearly see the streamlines being diverted from the leading edge region by the holes.

This figure though should not be interpreted to mean that there is no tip leakage around the holes because there is still some hot gas penetration into the region. We are only looking at streamlines released from a single plane upstream that allow us to obtain a general understanding of the flow. Looking at the large tip gap as shown in Figure (3 b) there is minimal effect on the mainstream flow patterns. Along the suction-side, just above the leading edge of the blade for the small tip gap notice the large number of streamlines that are not passing over the blade when compared to the large tip gap. Along the trailing edge pressure-side of the blade there is also a substantial number of streamlines that do not pass over the small tip when compared to the large tip.

Some interesting comparisons can be made between the two cases with holes blowing (Figure 3) and the four cases with blowing (Figure 4). The tip leakage vortex does not seem to change substantially with the holes blowing, but along the suction side of the blade just above the holes there is a noticeable change in the number of streamlines that are diverted into this area with the addition of blowing for a small tip gap.

Streamlines released from inside the plenum and colored by non-dimensional temperature are shown in Figure (4) for blowing levels of 1% and 2% at small and large tip gap heights. The high blowing ratio of 2% is presented in

$$= \frac{\partial}{\partial x}(\rho \frac{\partial \phi}{\partial x}) + \frac{\partial}{\partial y}(\rho \frac{\partial \phi}{\partial y}) + \frac{\partial}{\partial z}(\rho \frac{\partial \phi}{\partial z}) + S_{\phi} \dots (10)$$

In the present study, the (SIMPLE) algorithm (Semi-Implicit Method for Pressure Linked Equation) is used to couple the pressure and velocity as in Versteeg & Malalasekera [11].

### 3. COMPUTATIONAL METHODOLOGY

To better understand the effects of adiabatic effectiveness, a computational fluid dynamics (CFD) simulation was also performed. A commercially available CFD code, Fluent 6.3.26 [12] was used to perform all simulations. Fluent is a pressure based flow solver that can be used on unstructured grid that was used for the present study. All geometric construction and meshing were performed with GAMBIT 2.4.6. To ensure a high quality mesh, the flow passage was divided into multiple volumes, which allowed for more control during meshing. The tip gap region was of primary concern and was composed entirely of tetrahedral cells with an aspect ratio smaller than three. Inlet conditions to the model were set as a uniform inlet velocity. Figure (1) shows the mesh of the test rig. An inlet mass flow boundary condition was imposed for the coolant at the plenum entrance for the cooling holes.

To allow for reasonable computational times, all computations were performed using the RNG  $k-\epsilon$  turbulence model. Typical mesh sizes were composed of 4.8 million cells with

40% of the cells in holes and around the tip gap region. Typical computations required 2000 iterations for convergence.

### 4. GEOMETRY, FLOW AND BOUNDARY CONDITIONS

A Three-dimensional blade profile is created for these low speed. The scaling and design of blade profile and duct are discussed in Hohlfeld [4]. Table (2) lists the run conditions and input to the numerical simulations. The boundary condition on a blade surface assumes zero relative velocity between the blade surface and the shroud. All walls are adiabatic for adiabatic effectiveness cases. The main inlet is specified as a constant velocity inlet at 11.3 m/s. The inlet temperature in the duct ( $T_g$ ) is 750 K (taken from al-Dorah power station), the temperature that is used in cooling ( $T_c$ ) taken at 27 K and the pressure that used at atmosphere condition. The cooling holes locations is shown in Tables (3). The coordinate system is adjusted so that no coordinates are negative.

### 5. RESULTS AND DISCUSSION

Results are shown for cases with a baseline flat tip and coolant injection at a small and large tip gap (0.03 and 0.09 cm) respectively. blowing ratio ( $BR = U_{\infty}/U_c$ ) of 0.5%, 1%, 1.5% and 2% of the core inlet flow to explore thermal and flow effects within the passage. The results are presented in the dimensionless form of static pressure coefficient and

## 2. NUMERICAL ANALYSIS

The basic equations that describe the flow and heat transfer are conservation of mass, momentum and energy equations Arnal (10). The assumptions that used for the instantaneous equation are:-

- 1- Steady, 3D, incompressible flow, single phase flow, no slip.
- 2- The fluid is Newtonian.
- 3- Cartesian coordinate.

The basic equations according to Verestage and Malalasekera (11) that used in Fluent (12) program are:

Conservation of Mass

$$\partial/\partial x (\rho u) + \partial/\partial y (\rho v) + \partial/\partial z (\rho w) = 0 \dots (1)$$

Momentum Equations

u-momentum (x-direction)

$$\partial/\partial x (\rho u u) + \partial/\partial y (\rho u v) + \partial/\partial z (\rho u w) = -\partial p/\partial x + \partial/\partial x (\mu_{\text{eff}} \partial u/\partial x) + \partial/\partial y (\mu_{\text{eff}} \partial u/\partial y) + \partial/\partial z (\mu_{\text{eff}} \partial u/\partial z) + S_u \dots (2)$$

v-momentum (y-direction)

$$\partial/\partial x (\rho v u) + \partial/\partial y (\rho v v) + \partial/\partial z (\rho v w) = -\partial p/\partial y + \partial/\partial x (\mu_{\text{eff}} \partial v/\partial x) + \partial/\partial y (\mu_{\text{eff}} \partial v/\partial y) + \partial/\partial z (\mu_{\text{eff}} \partial v/\partial z) + S_v \dots (3)$$

w-momentum (z-direction)

$$\partial/\partial x (\rho w u) + \partial/\partial y (\rho w v) + \partial/\partial z (\rho w w) = -\partial p/\partial z + \partial/\partial x (\mu_{\text{eff}} \partial w/\partial x) + \partial/\partial y (\mu_{\text{eff}} \partial w/\partial y) + \partial/\partial z (\mu_{\text{eff}} \partial w/\partial z) + S_w \dots (4)$$

Energy Equation

$$\partial/\partial x (\rho u T) + \partial/\partial y (\rho v T) + \partial/\partial z (\rho w T) = \partial/\partial x (\Gamma_{\text{eff}} \partial T/\partial x) + \partial/\partial y (\Gamma_{\text{eff}} \partial T/\partial y) + \partial/\partial z (\Gamma_{\text{eff}} \partial T/\partial z) + S_T \dots (5)$$

The turbulence model utilized in this anal -

sis is the two equation k-Epsilon model. This model is utilized for its proven accuracy in turbine blade analysis and for its applicability to confined fluid flow. (k-ε) Turbulence Model is one of the most widely used turbulence models is the two-equation model of kinetic energy (k) and its dissipation rate (ε). The turbulence according to Launder and Spalding (13) is assumed to be characterized by its kinetic energy and dissipation rate (ε), where

Turbulence Energy, k

$$\partial/\partial x (\rho u k) + \partial/\partial y (\rho v k) + \partial/\partial z (\rho w k) = \partial/\partial x (\Gamma^k \partial k/\partial x) + \partial/\partial y (\Gamma^k \partial k/\partial y) + \partial/\partial z (\Gamma^k \partial k/\partial z) + G - \rho \epsilon \dots (6)$$

Energy Dissipation Rate, ε

$$\partial/\partial x (\rho u \epsilon) + \partial/\partial y (\rho v \epsilon) + \partial/\partial z (\rho w \epsilon) = \partial/\partial x (\Gamma^\epsilon \partial \epsilon/\partial x) + \partial/\partial y (\Gamma^\epsilon \partial \epsilon/\partial y) + \partial/\partial z (\Gamma^\epsilon \partial \epsilon/\partial z) + c_1 \epsilon/k G - c_2 \rho \epsilon^2/k \dots (7)$$

where

$$G = \mu_t \left[ 2 \left( \frac{\partial u}{\partial x} \right)^2 + \left( \frac{\partial v}{\partial y} \right)^2 + \left( \frac{\partial w}{\partial z} \right)^2 + 2 \left( \frac{\partial u}{\partial y} + \frac{\partial v}{\partial x} + \frac{\partial w}{\partial z} \right) \right] + S_G \dots (8)$$

$S_G$  given by Ideriah (14)

$$S_G = -2/3 \mu_t \left( \frac{\partial u}{\partial x} + \frac{\partial v}{\partial y} + \frac{\partial w}{\partial z} \right)^2 - 2/3 \rho k \left( \frac{\partial u}{\partial x} + \frac{\partial v}{\partial y} + \frac{\partial w}{\partial z} \right) \dots (9)$$

The values of the empirical constant used here are given in Table (1).

The governing equations (1), (2), (3), (4), (5), (6) and (7) can be written in one general form as shown below:

$$(\partial(\rho u \phi))/\partial x + (\partial(\rho v \phi))/\partial y + (\partial(\rho w \phi))/\partial z$$

by (100 c) results in average (50c) increased in blade temperature. The results also showed the temperature difference in blade metal of (250-450 c) between leading and trailing edges.

Fabien et al. [7] studied computationally a coupling strategy of a Navier Stokes flow solver and a conduction solver to predict blade temperature. The method is applied to the well documented NASA C3X configuration. The influence of the fluid/solid interface boundary condition is studied with regards to the wall temperature and heat flux prediction as well as to the computational efficiency. The predicted wall temperature is in good agreement with the experimental results. The method is finally applied to the prediction of the blade temperature of a high pressure turbine representative of a modern engine

Maosheng and Shusheng [8] investigated experimentally measurements of an active tip-clearance control method based on tip injection in a high-turning axial turbine cascade. Besides that, numerical investigations were also conducted to study phenomena which was not easily measured in the experiments. The results suggested that tip injection can weaken tip clearance flow, reducing the tip clearance mass flow and its associated losses. Meanwhile, the heat transfer condition on the blade tip surface can be also improved significantly. It also can be found that injection

chordwise location played an important role in the redistribution of secondary flow within the cascade passage.

Ahmed et al. [9] investigated numerically the optimization of film cooling parameters on a flat plate. They studied the effect of film cooling parameters such as inlet velocity direction, lateral and forward diffusion angles, blowing ratio, and streamwise angle on the cooling effectiveness, and optimum cooling parameters. The numerical simulation of the coolant flow through flat plate hole system is carried out using the "CFDRC package" coupled with the optimization algorithm "simplex" to maximize overall film cooling effectiveness. The results were compared with the published numerical and experimental data of a cylindrically round-simple hole, and the results show good agreement. In addition, the results indicated that the average overall film cooling effectiveness was enhanced by decreasing the streamwise angle for high blowing ratio and by increasing the lateral and forward diffusion angles.

The objective of the present work is to study the effect of blade tip and shelf on the adiabatic effectiveness of a turbine at different blowing ratios.



the gap, a smaller leakage vortex, and less aero losses in the tip gap.

Hohlfeld et al. (4) investigated computationally parasitic cooling flow losses, which are inherent to engines, and microcircuit channels. This study evaluated the benefit of external film-cooling flow exhausted from strategically placed microcircuits. Significant leading edge cooling was obtained from coolant exiting from dirt purge holes with a small tip gap while little cooling was seen with a large tip gap. Also the migration of coolant from the front leakage was shown to cool a considerable part of the platform. Several hot spots were predicted along the platform, which were circumvented through the placement of microcircuit channels. Ingestion of hot mainstream gas was predicted along the aft portion of the gutter and agreed with distress exhibited by actual gas turbine engines.

Christophel et al. (5) evaluated experimentally the adiabatic effectiveness levels that occur on the blade tip through blowing coolant from holes placed near the tip of a blade along the pressure side. A range of blowing ratios was studied by where coolant was injected from holes placed along the pressure side tip of a large scale blade model. Also he shows the dirt purge holes on the blade tip, which is part of a commonly used blade design to expel any large particles present in the coolant stream. Disregarding

the area cooled by the dirt purge holes, for a small tip gap the cooling holes provides relatively good coverage. For all of the cases considered, the cooling pattern is quite streaky in nature, indicating very little spreading of the jets. As the blowing ratio is increased for the small tip gap, there is an increase in the local effectiveness levels resulting in higher maxima and minima of effectiveness along the middle of the blade.

Adel H. Ayaal (6) studied computationally thermal analysis of a cooled turbine blade when the domain was divided into 3-regions. The first was the blade to blade passage (external flow) governed by quasi 3D Euler equations in a conservative form. A solution algorithm based on the finite difference McCormack's technique was used. The second region was the coolant passage (internal flow), 2D axisymmetric Naviers Stock equation was used. A solution algorithm based on the finite volume was staggered as a grid technique. The third region was blade metal to which a 3D Laplaces heat transfer equation is applied. The solution algorithm was based on the finite difference technique. The computational results showed that the blade surface (metal) temperature is cooler than the surrounding gases (external hot gases) by about (100-500°), depending on B.C. An increase in gas temperature by (100 °) results in (50-100°)increase in metal temperature. While the increased in coolant temperature



(adiabatic effectiveness) هدف هذا البحث هو حساب مستوى الذي يحدث على القمة والجذر للريشة من خلال نسب تبريد متغيرة باستخدام برنامج الفلونت. الدراسة النظرية انجزت في جريان بطيء مع فجوتان مختلفتان للقمة (0.03 و 0.09 سم) مع اختلاف نسب مائع التبريد من خلال ثقب (Blogging Ratios) لنسب النفث (film-cooling) التبريد الغشائي من خلال جريان مائع التبريد الذي يحقن من (Blogging Ratios) الثقب التي تقع على طول القمة لنموذج الريشة. رقم رينولد (2.1 × 105) أستعمل في الدراسة العددية. النتائج تبين افضل تبريد ينجز على الفجوة الصغيرة للقمة عند مقارنتها مع الفجوة الكبيرة للقمة مع اختلاف ظواهر الجريان التي تحدث في كل فجوة.

Keywords: heat transfer, film cooling and gas turbine.

## 1. INTRODUCTION

Gas turbine engines are widely used to power aircraft because they are light, compact and have a high power to-weight ratio. One way to increase power and efficiency of gas turbines is by increasing turbine-operating temperatures. The motivation behind this is that higher temperature gases yield higher energy potential. However, the components along the hot gas path experience high thermal loading, which can cause distress. The HPT (High Pressure Turbine) first stage blade is one component that is extremely affected by the hot gas.

Gas turbine blades usually have a gap between the blade tip and the stationary casing or the shroud surface known as tip gap. This clearance gap is necessary to allow for the blade's

mechanical and thermal growth. The leakage flow (flow through the tip gap) results in a reduction in the blade force, the work done and therefore the efficiency. This hot leakage flow also increases the thermal loading on the blade tip, leading to a high local temperature and thus, is considered as a primary source of blade failure. Metzger et al. (1).

The degree of cooling which may be achieved is dependent upon a number of factors (a) the temperature difference between the main gas stream and the inlet cooling air and (b) the conductance ratio this being defined as the ratio of the heat input to the blade per unit temperature difference between gas stream and blade to the heat passed to the cooling air per unit temperature difference between blade and cooling air. The heat input to the blade is dependent upon the blade shape, gas flow incidence, gas flow Reynolds number, gas Prandtl number, and to a lesser extent upon the ratio of gas temperature to blade temperature, and also gas stream Mach number. Jonas (2).

The work presented in this paper is concerned with the effects of injecting coolant to the tip of a turbine blade.

Tallman and Lakshminarayana (3) discusses tip leakage phenomena in turbines using a computational, pressure-correction based, three dimensional Navier-Stokes code. Their results showed that a reduced tip clearance results in less mass flow through

Dr. Ahmed F. Khudheyer

Mech. Eng. Dept.  
Al-Nahrain University

ahyaja@yahoo.com

Assest Lec. Hussein T. Dhaiban

Refrigeration and Air-conditioning Eng. Dept.  
Dijlah University College

husseinayo@gmail.com

## NUMERICAL STUDY OF THE EFFECT OF A BLADE TIP AND SHELF ON THE ADI - BATIC EFFECTIVENESS OF A TURBINE

### Abstract

Turbine airfoils are exposed to the hottest temperatures in the gas turbine with temperatures typically exceeding the melting point of the blade material. Cooling methods investigated in this computational study included cooling flow losses, which are inherent to engines. Film-cooling is one typically used cooling method whereby coolant is supplied through holes placed along the camber line of the blade.

The subject of this paper is to evaluate the adiabatic effectiveness levels that occur on the blade tip and shelf through blowing coolant ratio by using Fluent code. Numerical study are performed in a low speed with two different tip gaps (0.03 and 0.09 cm) and multipl

coolant flow rates through the film-cooling holes. A range of blowing ratios is studied whereby coolant injected from holes placed along the tip of a large scale blade model. The Reynolds number ( $2.1 \times 10^5$ ) is used in the numerical model. The results show much better cooling can be achieved for a small tip gap compared with a large tip gap with different flow phenomena occurring for each tip gap setting.

### الخلاصة

الشكل الانسيابي لريش للتوربين معرضة الى درجات حرارة عالية الى حد قد تتجاوز درجة انصهار معدن الريشة. انواع التبريد المفترضة في هذه الدراسة العددية بحيث تتضمن هو احد طرق (film-cooling) خسائر جريان التبريد التبريد النموذجية حيث ان مائع التبريد يجهز من خلال ثقبوب تقع على طول خط المنتصف لريشة التوربين.